Journal of Electronic Materials (2022) 51:3216–3225
https://doi.org/10.1007/s11664-022-09564-0

ORIGINAL RESEARCH ARTICLE

One-Step Synthesis of High-Purity and High-Aspect-Ratio Silver Nanowires by a Solvothermal Process with Mixed Polymer Capping Agents

Lei Hao[1] · Jian Wei[1] · Jiamin Wang[1,2] · Huan Su[1] · Congmin Qin[1] · Hao Zhang[1]

Received: 24 August 2021 / Accepted: 1 March 2022 / Published online: 25 March 2022

Abstract
Silver nanowires (AgNWs) with a high aspect ratio (>2000) have remarkable flexibility and photoelectric properties. Moreover, these nanowires are an important alternative for flexible transparent electrodes because of their significant electrical conductivity and low cost when fabricated into conductive networks on transparent substrates. Most reported AgNWs have low aspect ratios and are accompanied by numerous nanoparticles, which require an additional purification treatment. A one-step synthesis is still challenging for high-purity AgNWs with ultra-high aspect ratios (>2000), thin diameters, and few particle by-products. In this work, we propose a strategy to effectively improve the aspect ratio of AgNWs. We used a polyvinylpyrrolidone (PVP) mixture as the capping agent and explored the effects of mixing PVPs with two different molecular weights: 1,300,000 Da and 40,000 Da. The fabricated AgNWs are highly pure (AgNPs×100 < 0.29 pieces/square micron) with diameters of about 40 nm, an aspect ratio of more than 2000, and a quality factor of 7407.41. Thus, our strategy paves the way for low-cost and large-scale manufacturing of high-purity flexible transparent electronics.

Keywords Silver nanowires · solvothermal method · silver nanoparticles · polyvinylpyrrolidone

Introduction

A flexible transparent conductive electrode is a key element in many flexible optoelectronic devices, such as transparent fingerprint sensors,[1] touch screens,[2,3] LCDs,[4,5] and solar cells.[6] The tremendous growth of these devices has led to the demand for flexible conductive electrodes. Indium tin oxide (ITO) is the most important conductor for traditional optoelectronic devices. However, the ceramic brittleness of ITO limits its development into flexible conductive electrodes. This critical problem is being solved with the next generation of conductive electrodes, such as graphene,[7] conducting polymers,[8] metal nanowires (Ag, Au, and Cu),[5,9] and carbon nanotubes (CNTs).[10] Among these emerging candidates, metal nanowires are attracting increasing attention as an alternative flexible transparent conductor because of the low yield of graphene, the instability of conductive polymers, and the high levels of impurities and low dispersity of CNTs. Further considering the nature of metals (e.g., Au, Cu) and the production complexity, silver nanowires (AgNWs) are an excellent alternative to commercial ITO materials owing to their highest electrical conductivity among all relevant metals, good physical and chemical stability, and low cost.[11,12] Being a transparent electrode, AgNWs are also comparable to expensive ITO in terms of flexibility, transmittance, and electrical conductivity.[13] Currently synthesized AgNWs have a low aspect ratio, many silver nanoparticle (AgNP) by-products, and low purity. Numerous experiments have established that the synthesis of AgNWs with high aspect ratios effectively improves the optical transmittance[2,14] since large, optically transparent "holes" are formed between high-aspect-ratio metal nanowires,[15] which improves the electrode conductivity, and reduces both the sheet resistance and cost.

The liquid phase method using ethylene glycol as a solvent is the most promising method for AgNW synthesis, and there are many synthetic techniques, such as the polyol method,[13] solvothermal method,[16,17] DNA template

✉ Jian Wei
soonfound@163.com

[1] College of Materials Science and Engineering, Xi'an University of Architecture and Technology, Xi'an 710055, People's Republic of China

[2] China West Construction North Co., Ltd, Xi'an 710063, People's Republic of China

method,[18] and electrochemical deposition method.[19] Although the polyol method is a widely studied and mature process, its application has been limited because the AgNWs produced have a low aspect ratio[20–23] and are accompanied by many silver nanoparticles (AgNPs).[24–27] It is also difficult to control the AgNW purity and aspect ratio using the polyol method; therefore, high-quality AgNWs are produced but with poor repeatability.[26] Recently, Wang et al. described the use of the polyol method to synthesize silver nanowires with a diameter of 75 nm, an aspect ratio of only over 500, and 100 times the number of AgNPs in less than 4.14 pieces (PCS) per square micron (μm^2) after centrifugation for 5 min.[20] Meanwhile, Fang et al.[23] used a polyol method to synthesize AgNWs, which were purified by selective precipitation to obtain thick and long AgNWs with a diameter of 116 nm and an aspect ratio of 1200.

Compared with the polyol method, the solvothermal method shows strong advantages and is an ideal method to synthesize high-aspect-ratio AgNWs. Research has also focused on the synthesis of high-aspect-ratio AgNWs by the solvothermal method. In 2012, Zhu et al. used CuCl as the control agent in the hydrothermal reaction process, and further purification was performed to obtain AgNWs with a diameter of 20 nm, an aspect ratio of 1000, and AgNPs ×100 of less than 10.89 PCS/μm^2.[28] Then, in 2013, Lee and coworkers successfully synthesized AgNWs with AgNPs×100 below 184.71 PCS/μm^2 and further purified the nanowires to a diameter of about 20 nm and aspect ratio of about 1000 by a hydrothermal reactor, which uses NaCl and KBr as control agents.[29] Moreover, Ye et al. reported in 2017 the synthesis of ultra-long AgNWs (approximately 50 nm in diameter, 4000 aspect ratio, and unpurified AgNPs×100 < 1.22 PCS/μm^2) using a filter cloth after a hydrothermal reaction.[24] However, a one-step synthesis is still challenging for high-purity AgNWs with an ultra-high aspect ratio (>1500), thin diameter, and a small number of particle by-products.

In the conventional polyol method, AgNWs are synthesized by a continuous multi-step growth method using ethylene glycol as a solvent by adjusting the concentrations of polyvinylpyrrolidone (PVP), $AgNO_3$ and halide ions. PVP is widely known to play an important role as a stabilizer and capping agent during the growth of AgNWs.[30] PVP molecules with longer chains have stronger bond strength and have also been demonstrated to self-assemble into an ordered two-dimensional array on Ag nanocrystal surfaces.[31,32] At the same time, other studies have shown that PVP molecules with shorter chains have higher capping efficiency and incomplete coverage on the Ag seed surface, which leads to the anisotropic growth of Ag crystal nuclei.[33] Therefore, we employed a PVP mixture with different molecular weights (Mw, i.e., different chain lengths) as the capping agent to synthesize ultra-high-aspect-ratio (>1500) AgNWs. Moreover, AgNWs with a diameter of less than 40 nm and an aspect ratio of more than 1000 were reportedly synthesized by the PVP mixture.[25] Although the AgNWs fabricated by PVP mixture as the capping agent still has a relatively low aspect ratio, only a few nanoparticles emerged in the synthesized AgNWs, which demonstrates high purity. This is difficult to achieve by the traditional polyol method.

In this study, we propose a strategy that effectively improves the aspect ratio of AgNWs by incorporating PVP mixtures into the solvothermal process. Two PVP variants with different Mw were employed as capping agents in the solvothermal processes, which have not been investigated in previous reports. The solvothermal method easily synthesizes high-aspect-ratio AgNWs, and the PVP mixture allows for high-purity synthesis of AgNWs with few particle by-products. Therefore, combining the advantages of the solvothermal method and PVP mixing, it is easy to achieve AgNWs with high purity and high aspect ratios. A series of comparative experiments were designed to ascertain the delicate and distinctive roles of PVP molecular weights during the growth process of high-aspect-ratio AgNWs. The effect of reaction temperature and ferric chloride on the growth of high-aspect-ratio AgNWs was also investigated. The results of this study were also compared with those of previous reports on AgNW fabrication.

Experimental Section

Chemicals and Reagents

Commercial $AgNO_3$ (≥99.98% purity, Sinopharm Chemical Reagent Co., Ltd.), $FeCl_3$ (≥99.00% purity, Sinopharm Chemical Reagent Co., Ltd.), and ethylene glycol (EG, 99.98% purity, Sinopharm Chemical Reagent Co., Ltd.) were used in this work. PVP-1,300,000 Da (Mw = 1,300,000 Da, 99.98% purity) was purchased from Alfa Aesar (China, Grand Chemical Co., Ltd.) and PVP-K30 Da (Mw = 40,000 Da, 99.98% purity) was purchased from Macklin (Shanghai Maclean Biochemical Technology Co., Ltd.). All chemicals were used as received without any further purification.

Synthesis of Ag Nanowires

AgNWs were prepared through the solvothermal approach as follows. First, varying amounts of both PVP-K30 Da and PVP-1,300,000 Da from 0.1 to 0.5 g were added into the respective beakers with 50 ml EG to form homogeneous EG solutions with molecular weight ratios of the long- to short-chain PVPs as follows: 5:1, 2:1, 1:1, 1:2, and 1:5. $AgNO_3$ (0.2 g, 1.18 mM) was then completely dissolved in the EG solution. Afterward, 0.2 mL of another EG solution with 0.025–0.225 mM $FeCl_3$ was injected into the above EG solution. The mixture was then transferred into a 50 mL

Teflon-lined stainless-steel autoclave and heated in a resistance oven at 130°C for 8 h. Then, the precipitate was collected by centrifugation at 3000 rpm for 5 min and washed several times by acetone and ethanol to remove the residual PVP and impurities. Finally, the samples were dispersed in ethanol for further use.

Characterization

Scanning electron microscopy (SEM) images were taken with an SU8010 microscope (FE-SEM, Hitachi). Transmission electron microscopy (TEM) was conducted by a 200 kV Tecnai G2 F20 S-TWIN microscope. Powder x-ray diffraction (XRD) patterns were obtained on an x-ray diffractometer (XRD, Empyrean) with Cu Kα radiation at a scanning rate of 2°/min in the 2θ range of 5°–90°. Lastly, UV-visible extinction spectra were collected by UV-vis spectrophotometer (Nicolet Evolution 300) at room temperature with ethylene glycol as the reference solution.

Results and Discussion

The as-prepared and re-dispersed AgNWs in ethanol solutions showed a grayish-white color with no significant precipitation at the bottom of the glass bottle as displayed in the inset of Fig. 1a. A large number of filamentous materials was clearly observed in the suspension when the glass bottle was shaken. A representative SEM image (Fig. 1a) showed that uniform and ultra-long AgNWs were obtained without Ag crystals, indicating a successful one-pot synthesis of high-purity AgNWs without any additional purification process. Based on statistical analysis, the average length and diameter were approximately 90 nm and 40 nm, respectively. Figure 1b shows a TEM image of the AgNWs. On the other hand, no residual PVP layer was coated on the AgNWs.[34] The products were further characterized by high-resolution transmission electron microscopy (HRTEM) and selected-area electron diffraction (SAED) analyses. It is seen from the HRTEM image of the selected area with higher magnification in Fig. 1d that the regular spacing of the observed lattice planes is 2.37 Å, which is consistent with the separation of Ag (111) planes, suggesting AgNW growth along the [110] direction; the growth direction of the silver nanowire is perpendicular to this plane. From Fig. 1a and e, a clear diffraction pattern can be seen. Thus, based on the fundamentals of crystallography, the single-crystal structure of synthesized AgNWs is determined.[27,35,36]

Figure 2 shows the XRD pattern of the obtained nanowires after centrifugation. The five diffraction peaks agree well with the (111), (200), (220), (311), and (222) faces of the face-centered cubic Ag, and no other diffraction peak is observed. The synthesized AgNWs also have good crystallinity and high purity. Among the diffraction patterns, the (111) plane has the strongest diffraction peak, which implies that Ag atoms were preferentially deposited on the (111) plane, which led to the growth along the [110] direction.

To study the effect of mixing the two PVPs on the morphology of AgNWs, weight ratios of 5:1, 2:1, 1:1, 1:2, and 1:5 between PVP-1,300,000 Da and PVP-K30 Da were

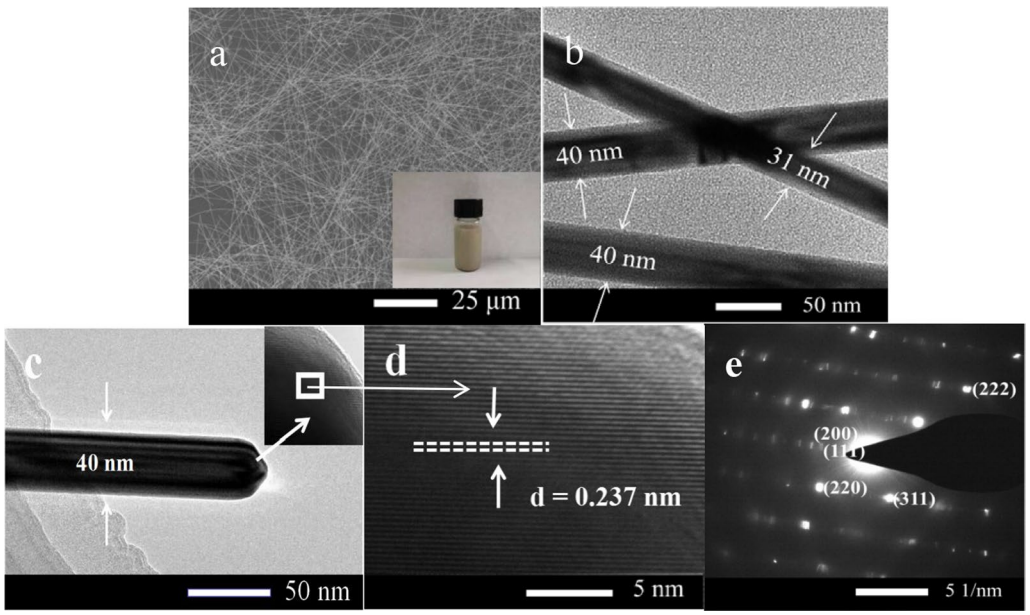

Fig. 1 (a) Low-magnification SEM image of the as-prepared AgNWs. Inset: camera picture of the AgNW suspension. (b, c) Typical TEM images of AgNWs, (d) the representative HRTEM image and (e) SAED image of AgNWs.

employed during the solvothermal reaction while keeping the other components and temperature unchanged. When the weight ratio was 5:1, we observed AgNPs (of approximately 200 nm in diameter) with a small amount of Ag nanorods as shown in Fig. 3a. When the ratio was reduced to 2:1 (Fig. 3b), longer silver nanowires were synthesized with a small number of particles. Moreover, when the ratio was 1:1, we synthesized Ag nanoparticles (of approximately 150 nm in diameter), and few nanorods as shown in Fig. 3c. In contrast, when the weight ratio was 1:2 (Fig. 3d), the density of silver nanoparticles increased (about 150 nm in diameter), and further adjusting the ratio to 1:5, the synthesized product was dominantly silver nanoparticles. Figure 4 summarizes the changes in Ag nanowire and nanoparticle diameters, and nanowire length as a function of the PVP weight ratio. The thin AgNWs are longest when the weight ratio of the two PVPs is 2:1. This was achieved by employing PVPs as the efficient capping agent essential for anisotropic growth of the Ag crystal nucleus. When PVP molecules with different chain lengths were mixed, short-chain molecules were adsorbed on the surface of the Ag seed and filled the gap between long-chain molecules, which effectively promotes the deposition of Ag ions on the (111) surface and the subsequent growth of AgNWs.

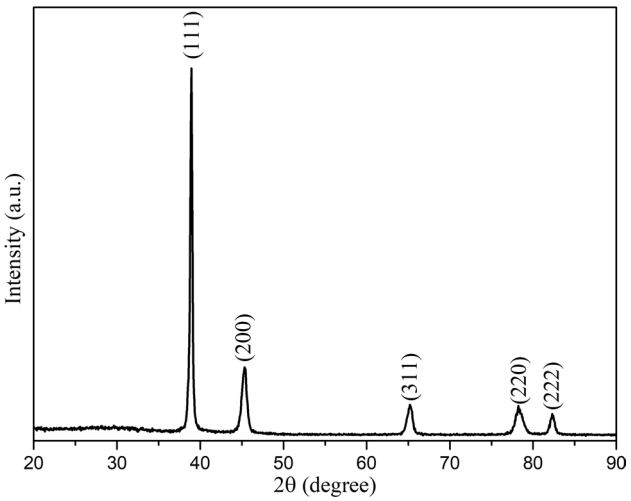

Fig. 2 Powder XRD pattern of the as-prepared AgNWs.

An optimized reaction temperature is also important and necessary for the formation of AgNWs in the solvothermal reaction. Figure 5 shows the SEM images of AgNWs synthesized under three solvothermal reaction temperatures. Stubby nanorods and particles were formed at a reaction temperature of 110°C (Fig. 5a) because the low temperature induced a slow reaction rate and caused isotropic growth of Ag crystal nucleus.[37] Meanwhile, small AgNPs began to dissolve into the reaction solution and were grown on the larger AgNPs by the Ostwald maturation process.[38,39] When the temperature was raised to 150°C (Fig. 5c), smaller nanoparticles were synthesized compared with those at 110°C (Fig. 5a). The higher temperature produced excessive energy which sped up the reaction rate of the solution; thus, the nucleation rate of the Ag crystal was higher than its growth rate. This produced a large number of AgNPs that were smaller than those formed at 110°C (Fig. 5a). It was only when the temperature was raised to 130°C (Fig. 5b) that the synthesized AgNWs dominated in numbers compared with nanoparticles. Therefore, we considered 130°C as the

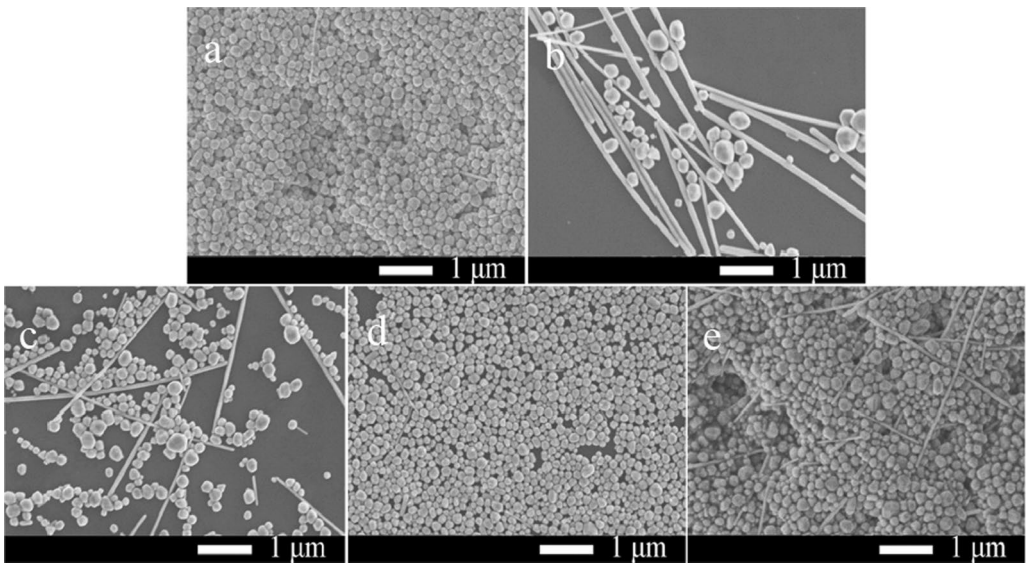

Fig. 3 FE-SEM images of AgNWs synthesized with weight ratio of PVP-1,300,000 Da and PVP-K30 Da of (a) 5:1, (b) 2:1, (c) 1:1, (d) 1:2, and (e) 1:5.

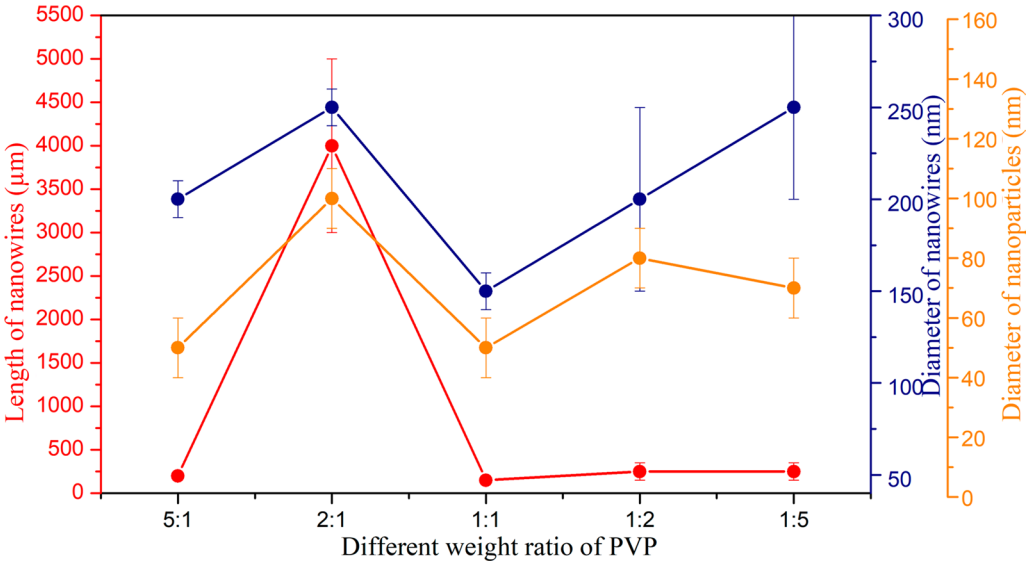

Fig. 4 Changes in nanowire/nanoparticle diameter and length as a function of the weight ratio of PVP-1,300,000 Da and PVP-K30 Da.

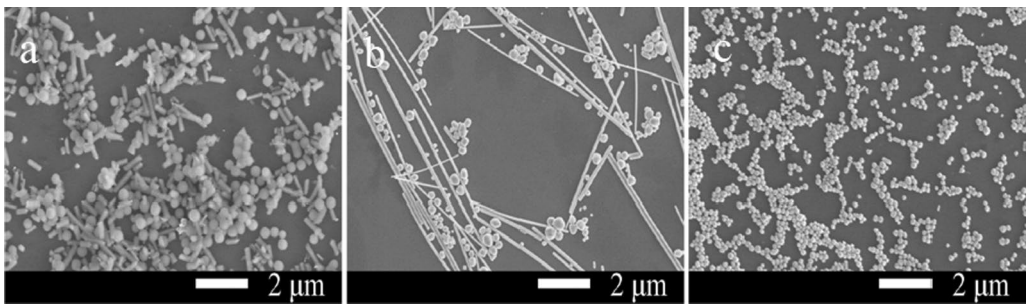

Fig. 5 SEM images of AgNWs synthesized at a reaction temperature of (a) 110°C, (b) 130°C, (c) 150°C (weight ratio of PVP-1,300,000 Da and PVP-K30 Da is 2:1).

appropriate temperature for the synthesis of high-aspect-ratio AgNWs. Meanwhile, the suitable temperature (130°C) also provided sufficient energy to promote the dissolution and formation of AgNPs, which modified and improved the growth of AgNWs.

$FeCl_3$ is widely known as a key control agent in the solvothermal synthesis of AgNWs.[40] Figure 6a, b, c, d, e, and f shows the SEM images of AgNWs synthesized at the $FeCl_3$ concentration of 0.025, 0.075, 0.125, 0.175, 0.200, and 0.225 mM, respectively, in another EG solution while keeping the weight ratio at 2:1 and the temperature at 130°C. Figure 6a shows that when the $FeCl_3$ concentration was 0.025 mM, the AgNWs had an average diameter of 200 nm, a length of 10 μm, and an aspect ratio of 50. When the concentration was 0.075 mM (Fig. 6b), the length and aspect ratio of the AgNWs increased to 30 μm and 200, respectively, while the diameter decreased to 150 nm. At $FeCl_3$ concentrations of 0.200 mM (Fig. 6e and f, respectively), the thinnest and longest AgNWs (about 40 nm in diameter, average 90 nm and largest 270 μm in length) were successfully achieved, which resulted in an average aspect ratio of more than 2000, with the largest aspect ratio at 6000. However, when the concentration was 0.225 mM (Fig. 6f), the synthesized AgNWs were accompanied by numerous large AgNPs. When the $FeCl_3$ concentration was less than 0.125 mM, the (100) plane of the Ag crystal nucleus was not adequately passivated, thus obtaining a mixture of AgNWs and their nanoparticle by-products. When the $FeCl_3$ concentration was more than 0.200 mM, many AgNPs were contained in the AgNWs. The high concentration of Cl^- increased the nucleation rate of the Ag atoms forming pentagonal twin seeds, deactivated the (100) surface of Ag, promoted the anisotropic growth of Ag atoms, and inhibited the radial growth of Ag atoms, which easily led to AgNP formation.[41] The dissolved oxygen in the solvent also facilitated the formation of AgNPs.[42,43] Figure 7 shows the diameter, length, and aspect ratio of AgNWs

as a function of $FeCl_3$ concentration. As the concentration of $FeCl_3$ increased, the AgNW diameter decreased, and the length and aspect ratio increased. When the $FeCl_3$ concentration was 0.200 mM, AgNWs had the thinnest diameter, the longest length, and the highest aspect ratio. Therefore, 0.200 mM was the optimal $FeCl_3$ concentration in EG solution for synthesizing thin and uniform high-aspect-ratio AgNWs with few particle by-products.

To clarify the growth mechanism of high-purity and high-aspect-ratio AgNWs, UV-Vis spectra and TEM measurement were employed. Figure 8 shows the UV-Vis spectra of seven time segments from the initial reaction time of 30 min to 8 h during the solvothermal synthesis. Meanwhile, Fig. 9 shows the corresponding TEM images of AgNWs in each time segment until 4 h. In the first 30 min of the reaction, we observed a wide and weak surface plasmon resonance (SPR) peak around a wavelength of 425 nm as shown in Fig. 8. The corresponding TEM image of the products (Fig. 9a) indicates that only 50–100 nm pentagonal twin structure AgNPs emerged.

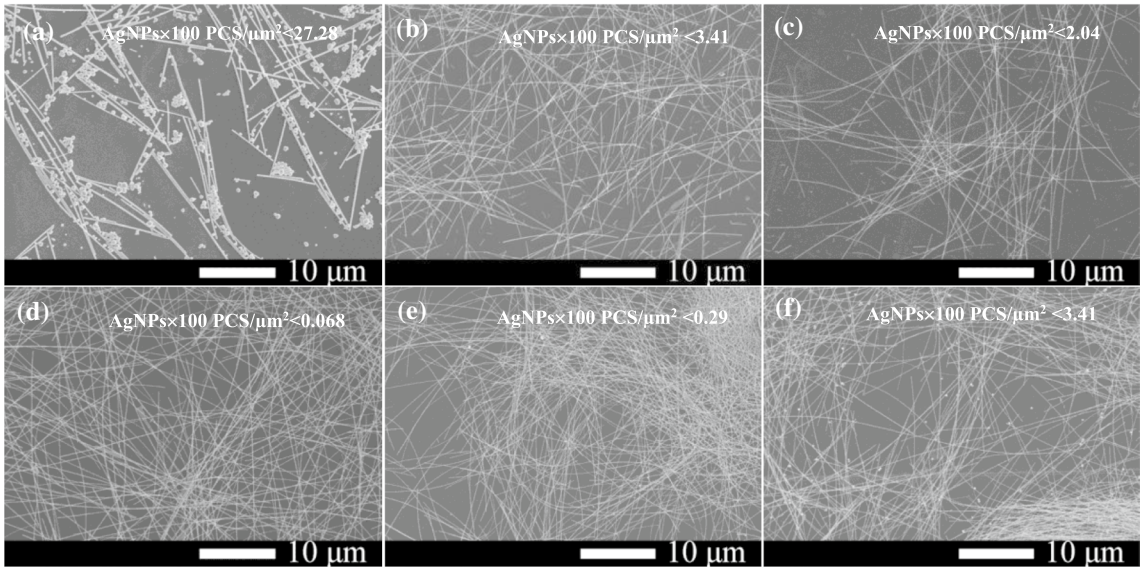

Fig. 6 $FeCl_3$ effect on the synthesis of AgNWs in the solvothermal reaction. (a) 0.025 mM, (b) 0.075 mM, (c) 0.125 mM, (d) 0.175 mM, (e) 0.200 mM, and (f) 0.225 mM. The diameter of AgNWs decreased with the increasing concentration of $FeCl_3$ from (a) to (f). The AgNPs×100 PCS/μm^2 decreased first and then increased with the increasing concentration of $FeCl_3$ from (a) to (f).

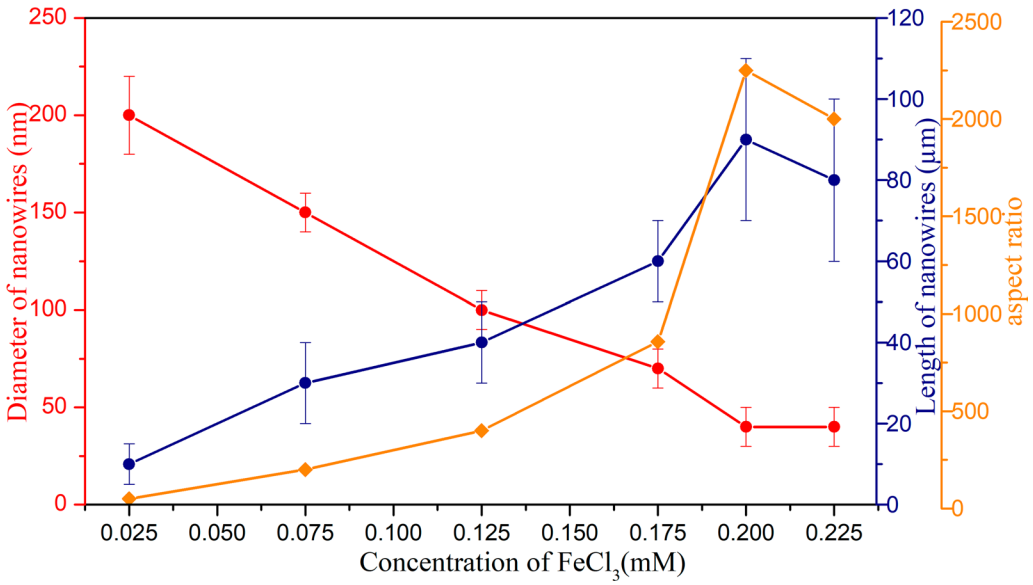

Fig. 7 Changes in nanowire diameter, length, and aspect ratio as a function of the $FeCl_3$ concentration.

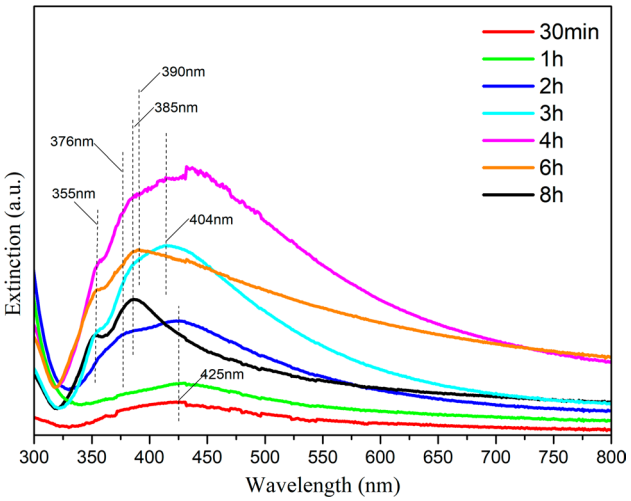

Fig. 8 Extinction spectra recorded from an aqueous suspension of products at different time segments from initial reaction time of 30 min to 8 h in the solvothermal synthesis process.

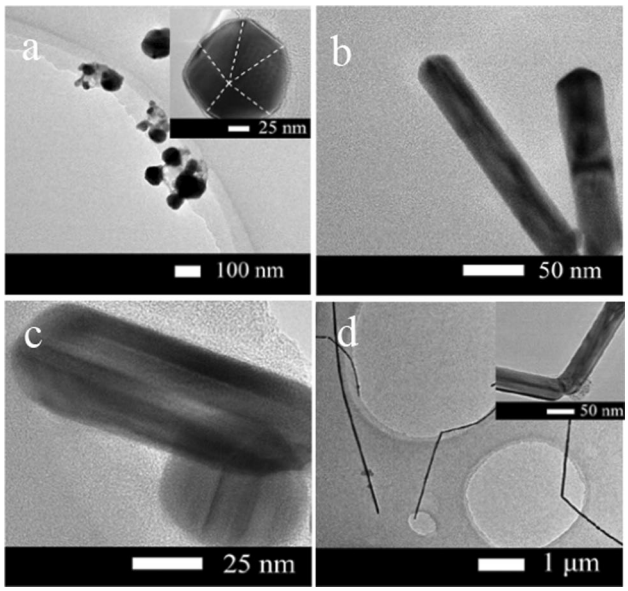

Fig. 9 TEM images of Ag seeds generated in (a) initial 30 min, (b) 1 h, (c) 2 h, and (d) 4 h. The inset in (a) is an HRTEM image of a pentagonal structure Ag seed with five (111) faces at one end. The inset in (d) is the image of a V-shaped nanowire.

During the 1–2 h period, an important transition from nanoparticles to nanorods was observed. Therefore, the SPR peak at 376 nm can be considered as an optical feature of the growth of nanoparticles into Ag nanorods. The nanowire TEM images of 1 and 2 h were decahedral rod-like structures, as shown in Fig. 9b and c. As the reaction time proceeded for 3–4 h, the Ag nanorods were completely converted into AgNWs (Fig. 9d). For the subsequent reaction time until 8 h, the AgNWs gradually grew, and their aspect ratio further increased. The three peaks at 355, 385, and 404 nm were observed to exist simultaneously from the UV-visible absorption spectrum for 3–4 h. When the reaction proceeded to 3 h, a new extinction peak was observed at 355 nm, a peak at 425 nm was gradually redshifted to 404 nm, and a peak at 376 nm was blueshifted to 385 nm. The peaks at 355 nm and 385 nm were similar to the transverse plasmonic peaks of the commonly observed pentagonal cross-section of nanorods.[38,44] The peak at 404 nm indicates an increase in the number of Ag nanorods.[20] When the reaction time was further increased to 6 h and 8 h, the SPR peak intensity decreased and the width became narrow. The peak at 355 nm indicates an increase in the number and length of nanowires and a decrease in the number of Ag nanoparticles. At 6 h, the peak at 404 nm representing the Ag nanorod completely disappeared. As the reaction progressed to 8 h, the length of AgNWs was further increased, and the number of AgNPs was further reduced. The redshift of the SPR peak at 390 nm to 385 nm is related to the tip of the AgNWs. The two SPR peaks at the last 355 and 385 nm are attributed to the fivefold twin structure of the AgNWs. Owing to the high aspect ratio of the synthesized AgNWs, their longitudinal plasma vibration peaks should be in the infrared region.[26] The inset image of Fig. 9d shows a V-shaped AgNW which is joined together at the nanowire end. It can be interpreted as the formation of a new pentagonal crystal structure on the (111) face of one AgNW end face, which formed after a reaction time of more than 4 h.[45]

Figure 10 shows the proposed growth mechanism of the synthesized AgNWs via the solvothermal method. The synthesis mechanism of high-purity and high-aspect-ratio AgNWs was attributed to the effect of temperature, the synergistic effect of PVP mixture (PVP-1,300,000 Da and PVP-K30 Da), and the promotion of NO^{3-}.

During the reaction, the temperature provides sufficient energy to promote the dissolution of AgNPs, which leads to more Ag^{+} and small AgNPs in the solution. Moreover, the temperature required for secondary nucleation is higher than the temperature at which AgNWs grow. Then, the secondary nucleation of AgNPs can be inhibited by controlling the synthesis temperature of the system, thereby achieving fewer AgNPs in the product.

Because of the high degree of polymerization of long-chain PVP, the presence of polycarbonyl groups can form Ag-O bonds with the (100)-faced Ag^{+}, which limits the lateral growth of Ag seeds.[46] Because of the large intermolecular forces (steric and repulsive forces) between the long-chain PVPs, it is difficult to closely align PVP on the (100) surface of Ag seeds.[33,41] Meanwhile, short-chain PVPs with small intermolecular forces are adsorbed on the (100) side of Ag seeds, filling the gap between the long-chain PVP molecules.[25] The strong chemical interaction between the PVP and (100) faces hinders the lateral growth of AgNWs,

while the weak interaction between the PVP and (111) faces results in the continuous growth of silver nanostructures along the elongated axis [110].[46] Therefore, some nanowires gradually grow into high-aspect-ratio AgNWs under the synergistic effect of PVPs. Part of the AgNWs form high-aspect-ratio AgNWs in the presence of high concentrations of nitrate anions by self-assembled growth mechanisms. Both Cl^-/O^{2-} and Cl^-/Fe^{3+} have strong corrosive effects on the surface of the AgNWs, resulting in a small AgNW diameter, a rough surface, and a prolonged reaction time.[47] In addition, the PVP-NO^{3-}-AgCl binding site, produced by the synergistic electrostatic interaction between NO^{3-} and AgCl, NO^{3-} and PVP, can be used as an attachment template between the ends of AgNWs.[48] AgNWs activate the ends by absorbing small AgNPs and extend themselves by attaching other AgNWs.[49] Owing to the thermodynamic stability of the nanowires, the curved V-shaped nanowires become straight, thereby obtaining ultra-long AgNWs with a pentagonal cross section.[45]

Figure 11 compares our present work with previous reports. The aspect ratio (Fig. 11a) of AgNWs in this study reached a high value of approximately 2000, which is second only to that reported by Ye. Meanwhile, Fig. 11b compares the unpurified AgNPs per square micron between our result and that of other studies. Considering the two factors of the diameter of AgNWs and the number of particles per square micron, the red circle in Fig. 11b represents AgNWs synthesized by the solvothermal method. Its value is more concentrated, the coordinates are closer to the origin, and the comprehensive value is lower than the value of the green circle, which was synthesized by the polyol method. The lowest content of unpurified AgNPs per square micron in this work was 0.29. Figure 12 shows a comparison of the quality factor of our results with that of other studies. We estimated the quality factor of AgNWs as the ratio of the AgNW aspect ratio to the 100-fold unpurified number of AgNPs per square micron. The quality factor of 7407.41 for this work is the highest in Fig. 12. Therefore, compared with

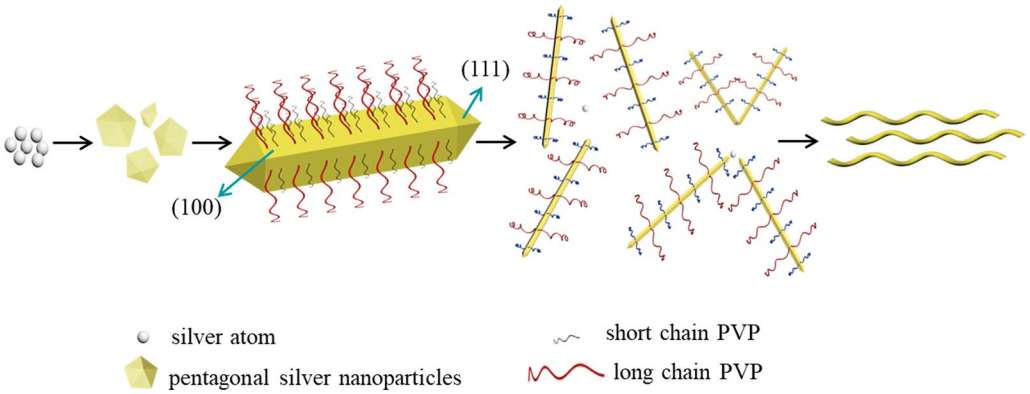

Fig. 10 The growth mechanism of AgNWs using mixed PVP molecules.

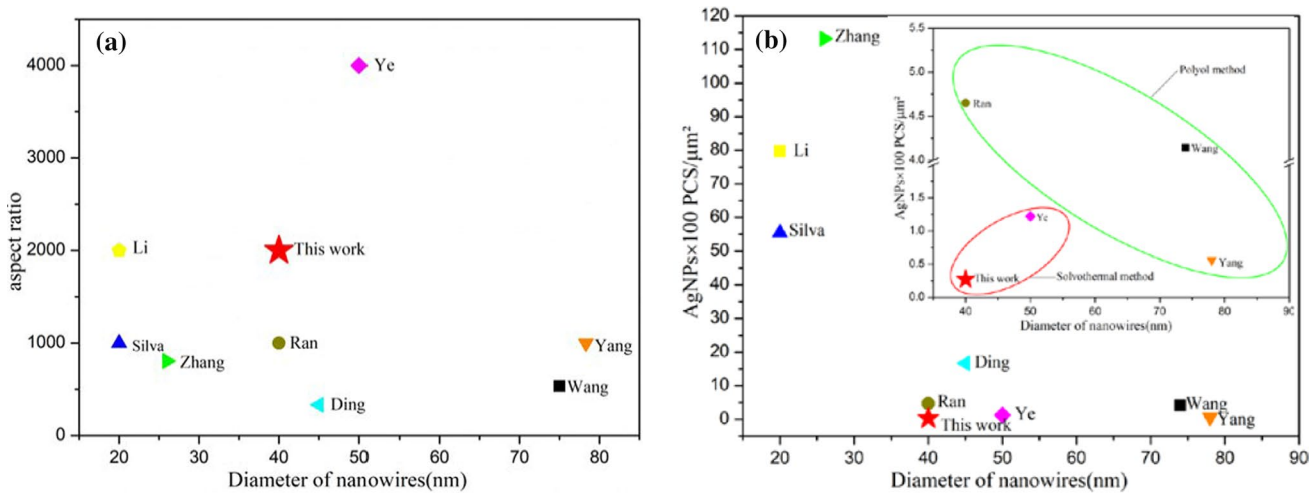

Fig. 11 (a) Comparison with other work in diameter and aspect ratio, (b) comparison with other work in diameter and AgNPs×100 PCS/μm^2 (square micron), (Ye,[24] Ran,[25] Silva,[26] Li,[27] Zhang,[50] Wang,[20] Yang,[51] Ding[52]).

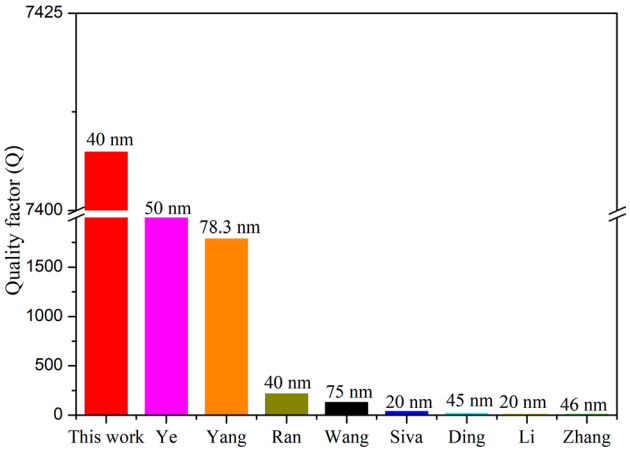

Fig. 12 Quality factor comparison of our work with other reports (Ye [24] Ran,[25] Silva,[26] Li,[27] Zhang,[50] Wang,[20] Yang,[51] Ding,[52]).

other studies, our work has the lowest content of unpurified AgNPs per square micron and the highest quality factor. The lowest content of unpurified AgNPs indicates the feasibility of the one-step synthesis of AgNWs, which greatly reduces industrial production cost.

Conclusions

Compared with the previous method of synthesizing AgNWs, we propose a simple and effective solvothermal method using two different PVPs as the control agent to synthesize AgNWs with a diameter of 40 nm, an aspect ratio of more than 2000, and a yield that was kept at about 80%. Owing to the presence of complexes (Ag^{+} combined with capping agent PVP) and NO^{3-}, the lateral growth of AgNWs was restricted and the nanowires only grew along the elongated axis. Finally, high-purity (AgNPs×100<0.29 PCS/μm^2), high-aspect-ratio (>2000), and high-quality-factor (7407.41) AgNWs with a pentagonal cross section were fabricated. The high-aspect-ratio and high-purity AgNWs are suitable in flexible transparent electrodes and in a variety of optoelectronic nanodevices. Our method paves the way for a low-cost and large-scale fabrication of such devices.

Acknowledgments This project was supported by the Natural Science Basic Research Plan in Shaanxi Province of China (Program No. 2017ZDJC-18), National Natural Science Foundation of China (Grant nos. 51308447, 51578448), and the Technology Foundation for Selected Overseas Chinese Scholar, Ministry of Human Resources and Social Security of the People's Republic of China (Shan Ren She Han [2016]789).

Conflict of interest The authors declare no conflict of interest in this study.

References

1. B.W. An, S. Heo, S. Ji, F. Bien, and J.U. Park, Transparent and flexible fingerprint sensor array with multiplexed detection of tactile pressure and skin temperature. *Nat. Commun.* 9, 2458 (2018).
2. B. Bari, J. Lee, T. Jang, P. Won, S.H. Ko, K. Alamgir, M. Arshad, and L. Guo, Simple hydrothermal synthesis of very long and thin silver nanowires and their application in high quality transparent electrodes. *J. Mater. Chem.* 4, 11365 (2016).
3. M. Vosgueritchian, D.J. Lipomi, and Z. Bao, Highly conductive and transparent PEDOT:PSS films with a fluorosurfactant for stretchable and flexible transparent electrodes. *Adv. Funct. Mater.* 22, 421 (2012).
4. S. Lin, Z. Wang, Y. Zhang, Y. Huang, R. Yuan, W. Xiang, and Y. Zhou, Easy synthesis of silver nanoparticles-orange emissive carbon dots hybrids exhibiting enhanced fluorescence for white light emitting diodes. *J. Alloys Compd.* 700, 75 (2017).
5. Y. Shengrong, A.R. Rathmell, C. Zuofeng, I.E. Stewart, and B.J. Wiley, Metal nanowire networks: the next generation of transparent conductors. *Adv. Mater.* 26, 6670 (2015).
6. Y. Zhang, Z. Sun, S. Cheng, and F. Yan, Plasmon-induced broadband light-harvesting for dye-sensitized solar cells using a mixture of gold nanocrystals. *Chemsuschem* 9, 813 (2016).
7. P. Jang-Ung, N. Sungwoo, L. Mi-Sun, and C.M. Lieber, Synthesis of monolithic graphene-graphite integrated electronics. *Nat. Mater.* 11, 120 (2011).
8. Y. Zhang, J. Guo, D. Xu, Y. Sun, and F. Yan, One-pot synthesis and purification of ultralong silver nanowires for flexible transparent conductive electrodes. *ACS Appl. Mater. Interfaces* 9, 25465 (2017).
9. C. Mayousse, C. Celle, A. Carella, and J. Pierre, Simonato, Synthesis and purification of long copper nanowires. Application to high performance flexible transparent electrodes with and without PEDOT:PSS. *Nano Res.* 7, 315 (2014).
10. B.S. Shim, J. Zhu, E. Jan, K. Critchley, and N.A. Kotov, Transparent conductors from layer-by-layer assembled SWNT films: importance of mechanical properties and a new figure of merit. *ACS Nano* 4, 3725 (2010).
11. Z. Teymouri, L. Naji, and Z. Fakharan, The influences of polyol process parameters on the optoelectronic characteristics of AgNWs-based flexible electrodes and their application in ITO-free polymer solar cells. *Org. Electron.* 62, 621 (2018).
12. M. Manceau, D. Angmo, and M. Jørgensen, ITO-free flexible polymer solar cells: from small model devices to roll-to-roll processed large modules. *Organic Electron.* 12, 566 (2011).
13. S.W. Hsu and A.R. Tao, Halide-directed synthesis of square prismatic Ag nanocrystals by the polyol method. *Chem. Mater.* 30, 4617 (2018).
14. R.M. Mutiso, M.C. Sherrott, A.R. Rathmell, B.J. Wiley, and K.I. Winey, Integrating simulations and experiments to predict sheet resistance and optical transmittance in nanowire films for transparent conductors. *ACS Nano* 7, 7654 (2013).
15. S.M. Bergin, C. Yu-Hui, A.R. Rathmell, C. Patrick, L. Zhi-Yuan, and B.J. Wiley, The effect of nanowire length and diameter on the properties of transparent, conducting nanowire films. *Nanoscale* 4, 1996 (2012).
16. Z. Wang, J. Liu, X. Chen, J. Wan, and Y. Qian, A simple hydrothermal route to large-scale synthesis of uniform silver nanowires. *Chem.–Eur. J.* 11, 160 (2005).
17. X. M. Sun and Li. Y. D, Cylindrical silver nanowires: preparation, structure, and optical properties. *Adv. Mater,* 17, 2626 (2005).
18. Y.W. Cao, R. Jin, and C.A. Mirkin, DNA-modified core-shell Ag/Au nanoparticles. *J. Am. Chem. Soc.* 123, 7961 (2001).
19. J. Low, S. Qiu, D. Xu, C. Jiang, and B. Cheng, Direct evidence and enhancement of surface plasmon resonance effect on Ag-loaded

TiO_2 nanotube arrays for photocatalytic CO_2 reduction. *Appl. Surf. Sci.* 423 (2018).
20. S. Wang, Y. Tian, D. Su, and Y. Huang, Rapid synthesis of long silver nanowires by controlling concentration of Cu^{2+} ions. *Mater. Lett.* 172, 175 (2016).
21. D.S. Hecht, H. Liangbing, and I. Glen, Emerging transparent electrodes based on thin films of carbon nanotubes, graphene, and metallic nanostructures. *Adv. Mater.* 23, 1482 (2011).
22. Z. Pei, I. Wyman, J. Hu, S. Lin, Z. Zhong, Y. Tu, Z. Huang, and Y. Wei, Silver nanowires: synthesis technologies, growth mechanism and multifunctional applications. *Mater. Sci. Eng.* B, 223, 1 (2017).
23. Y. Fang, Z. Wu, L. Jia, F. Jiang, and B. Hu, High-performance hazy silver nanowire transparent electrodes through diameter tailoring for semitransparent photovoltaics. *Adv. Funct. Mater.* 28, 1705409 (2018).
24. Z. Ye, J. Guo, X. Dan, S. Yi, Y. Feng, Z. Ye, J. Guo, X. Dan, S. Yi, and Y. Feng, One-pot synthesis and purification of ultralong silver nanowires for flexible transparent conductive electrodes. *ACS Appl. Mater. Interfaces* 9, 25465 (2017).
25. R. Yunxia, H. Weiwei, W. Ke, J. Shulin, and Y. Changhui, A one-step route to Ag nanowires with a diameter below 40 nm and an aspect ratio above 1000. *Chem. Commun.* 50, 14877 (2014).
26. R.R. Silva, M. Yang, S.I. Choi, M. Chi, M. Luo, C. Zhang, Z.Y. Li, P.H. Camargo, S.J. Ribeiro, and Y. Xia, Facile synthesis of sub-20 nm silver nanowires through a bromide-mediated polyol method. *ACS Nano* 10, 7892 (2016).
27. B. Li, S. Ye, I.E. Stewart, S. Alvarez, and B.J. Wiley, Synthesis and purification of silver nanowires to make conducting films with a transmittance of 99%. *Nano Lett.* 15, 6722 (2015).
28. Z. Gang and D. Chen, Solvothermal fabrication of uniform silver nanowires. *J. Mater. Sci.: Mater. Electron.* 23, 2035 (2012).
29. E.-J. Lee, M.-H. Chang, Y.-S. Kim, and J.-Y. Kim, High-pressure polyol synthesis of ultrathin silver nanowires: electrical and optical properties high-pressure polyol synthesis of ultrathin silver nanowires: electrical and optical properties. *APL Mater.* 1, 273 (2013).
30. Y. Borodko, S.M. Humphrey, T.D. Tilley, H. Frei, and G.A. Somorjai, Charge-transfer interaction of poly(vinylpyrrolidone) with platinum and rhodium nanoparticles. *J. Phys. Chem. C* 111, 6288 (2007).
31. J.J. Zhu, C.X. Kan, J.G. Wan, M. Han, and G.H. Wang, High-yield synthesis of uniform Ag nanowires with high aspect ratios by introducing the long-chain PVP in an improved polyol process. *J. Nanomater* 2011, 982547 (2011).
32. X. U. Li-Hong, C. X. Kan, C. S. Wang, B. Cong, N. I. Yuan, and D. N. Shi, Synthesis of Ag nanostructures with controlled shapes by a polyvinylpyrrolidone-assisted hydrothermal method. *Acta Phys.-Chim. Sin.* 30, 569 (2014).
33. X.X. Hu, Z. Jie, O.L. Kyle, L.Q. Ge, and X.Y. Nan, Quantitative analysis of the role played by poly(vinylpyrrolidone) in seed-mediated growth of Ag nanocrystals. *J. Am. Chem. Soc.* 134, 1793 (2012).
34. G. Sang, Y. Cao, M. Fan, G. Lu, Y. Zhu, Q. Zhao, and X. Cui, Development of a novel sulphoalumitate cement-based composite combing fine steel fibers and phase change materials for thermal energy storage. *Energy Build.* 183, 75 (2019).
35. H. Yang, T.R. Chen, H.F. Wang, S.C. Bai, and X.Z. Guo, One-pot rapid synthesis of high aspect ratio silver nanowires for transparent conductive electrodes. *Mater. Res. Bull.* 102, 79 (2018).
36. X.W. Meng, Y.Y. Mao, Y.W. Yang, H.W. Yang, C.Y. Hu, J.M. Guo, and Y.Q. Li, Synthesis of ultra-long silver nanowires by SNS-directed method and their characterization. *Precious Metals.* 38, 20 (2017).
37. H. Wang, B.K. Li, C. Xu, S.C. Xu, and G.H. Li, Large-scale solvothermal synthesis of Ag nanocubes with high SERS activity. *J. Alloys Compd.* 772, 150 (2019).
38. Y. Sun, B. Gates, B. Mayers, and Y. Xia, Crystalline silver nanowires by soft solution processing. *Nano Lett.* 2, 165 (2002).
39. Y. Sun, B. Mayers, T. Herricks, and Y. Xia, Polyol synthesis of uniform silver nanowires: a plausible growth mechanism and the supporting evidence. *Nano Lett.* 3, 955 (2003).
40. D. Chen, X. Qiao, X. Qiu, J. Chen, and R. Jiang, Large-scale synthesis of silver nanowires via a solvothermal method. *J. Mater. Sci.: Mater. Electron.*, 22, 6 (2011).
41. K. Zhan, R. Su, S. Bai, Z. Yu, N. Cheng, C. Wang, S. Xu, W. Liu, S. Guo, and Z.X. Zhao, One-pot stirring-free synthesis of silver nanowires with tunable lengths and diameters via a Fe(3+) & Cl(-) co-mediated polyol method and their application as transparent conductive films. *Nanoscale* 8, 18121 (2016).
42. Y. Zheng, J. Zeng, A. Ruditskiy, M. Liu, and Y. Xia, Oxidative etching and its role in manipulating the nucleation and growth of noble-metal nanocrystals. *Chem. Mater.* 26, 22 (2013).
43. B. Wiley, T. Herricks, Y. Sun, and Y. Xia, Polyol synthesis of silver nanoparticles: use of chloride and oxygen to promote the formation of single-crystal. *Truncated Cubes Tetrahedrons. Nano Lett.* 4, 1733 (2004).
44. Y. Sun, Y. Yin, B.T. Mayers, T. Herricks, and Y. Xia, Uniform silver nanowires synthesis by reducing $AgNO_3$ with ethylene glycol in the presence of seeds and poly(vinyl pyrrolidone). *Chem. Mater.* 14, 4736 (2002).
45. Z. Shu-Hong, J. Zhi-Yuan, X. Zhao-Xiong, X. Xin, H. Rong-Bin, and Z. Lan-Sun, Growth of silver nanowires from solutions: a cyclic penta-twinned-crystal growth mechanism. *J. Phys. Chem. B* 109, 9416 (2005).
46. H.H. Huang, X.P. Ni, G.L. Loy, C.H. Chew, K.L. Tan, F.C. Loh, J.F. Deng, and G.Q. Xu, Photochemical formation of silver nanoparticles in poly(N-vinylpyrrolidone). *Langmuir* 12, 909 (1996).
47. E.C. Dong, Rapid production of silver nanowires based on high concentration of $AgNO_3$ precursor and use of $FeCl_3$ as reaction promoter. *RSC Adv.* 4, 21060 (2014).
48. K. Chien Lin, and H. Kuo Chu, Nitrate ion promoted formation of Ag nanowires in polyol processes: a new nanowire growth mechanism. *Langmuir* 28, 3722 (2012).
49. M. Hu, J. Gao, Y. Dong, S. Yang, and R.K.Y. Li, Rapid controllable high-concentration synthesis and mutual attachment of silver nanowires. *RSC Adv.* 2, 2055 (2012).
50. K. Zhang, Y. Du, and S. Chen, Sub 30 nm silver nanowire synthesized using KBr as co-nucleant through one-pot polyol method for optoelectronic applications. *Org. Electron.* 26, 380 (2015).
51. Y. Hui, T. Chen, H. Wang, S. Bai, and X. Guo, One-pot rapid synthesis of high aspect ratio silver nanowires for transparent conductive electrodes. *Mater. Res. Bull.* 102, 79 (2018).
52. H. Ding, Y. Zhang, G. Yang, S. Zhang, L. Yu, and P. Zhang, Large scale preparation of silver nanowires with different diameters by a one-pot method and their application in transparent conducting films. *RSC Adv.* 6, 8096 (2016).